Biochemical and Biophysical Research Communications 432 (2013) 539–544

Contents lists available at SciVerse ScienceDirect

Biochemical and Biophysical Research Communications

journal homepage: www.elsevier.com/locate/ybbrc

Prion protein conversion induced by trivalent iron in vesicular trafficking

Bo-Ran Choi [a], Jeongmin Lee [a,b], Su Yeon Kim [b], Inbeen Yim [a], Eun-Hee Kim [a], Hee-Jong Woo [a,*]

[a] Laboratory of Immunology, College of Veterinary Medicine, Seoul National University, Seoul 151-742, Korea
[b] Division of Zoonoses, Center for Immunology and Pathology, National Institute of Health, Korea Centers for Disease Control and Prevention, Cheongwon-gun, Chungcheongbuk-do 363-951, Korea

ARTICLE INFO

Article history:
Received 29 January 2013
Available online 14 February 2013

Keywords:
Prion protein conversion
Iron
Proteinase K resistance
Vesicular trafficking
Lysosomes

ABSTRACT

Iron dyshomeostasis has been observed in prion diseases; however, little is known regarding the contribution of the oxidation state of iron to prion protein (PrP) conversion. In this study, PrP^C-deficient HpL3-4 cells were exposed to divalent [Fe(II)] or trivalent [Fe(III)] iron, followed by exogenous recombinant PrP (rPrP) treatment. We then analyzed the accumulation of internalized rPrP and its biochemical properties, including its resistance to both proteinase K (PK) digestion and detergent solubility. Fe(III), but not Fe(II), induced the accumulation of internalized rPrP, which was partially converted to detergent-insoluble and PK-resistant PrP (PrP^{res}). The Fe(III)-induced PrP^{res} generation required an intact cell structure, and it was hindered by U18666A, an inhibitor of vesicular trafficking, but not by NH_4Cl, an inhibitor of endolysosomal acidification. These observations implicated that the Fe(III)-mediated PrP^{res} conversion likely occurs during endosomal vesicular trafficking rather than in the acidic environment of lysosomes.

1. Introduction

Fatal neurodegenerative disorders associated with prion protein (PrP) occur in many vertebrates: Creutzfeldt–Jakob disease (CJD) in humans, bovine spongiform encephalopathy (BSE) in cattle, scrapie in sheep, and chronic wasting disease (CWD) in deer and elk. The central event in all prion diseases is the conversion of the alpha-helix-rich form of PrP (cellular PrP; PrP^C) to a beta-sheet-rich form (PrP scrapie; PrP^{Sc}); the accumulation of PrP^{Sc} is believed to be a causative factor of neurotoxicity in prion diseases [1]. In prion-infected brains, metal homeostasis imbalance and associated oxidative stress have been found and are considered triggers of neurotoxicity [2,3]. Although the functional roles for PrP^C have not been clearly identified, a relationship with metal homeostasis, including iron and copper homeostasis, has been proposed [4,5]. In the disease state, the iron content increases in the cerebral cortex, striatum, and brain stem of scrapie-infected mice [4]; however, copper levels are reduced [6]. Although a relationship between redox-iron and PrP accumulation has been observed [4,7], the factor(s) and mechanism(s) for PrP alteration associated with redox-iron accumulation remain to be determined. The effects of iron on the aggregation of PrP^C and the neurotoxicity associated with the aggregated PrP have been studied in neuroblastoma cells that overexpress PrP^C [8–10]. However, the relative contribution of the 2 states of iron (divalent [Fe(II)] and trivalent [Fe(III)] iron) to the generation of abnormal PrP isoforms has not been determined. In addition, the intracellular sites and mechanism of iron-mediated PrP conversion remain to be investigated, although several studies have proposed that the cell surface, endosomes, and acidic lysosomes are all potential PrP conversion sites, owing to the cellular localization of disease-associated isoforms [11,12].

In this study, cells devoid of endogenous PrP^C were overloaded with iron and treated with recombinant bovine PrP (rPrP). We exploited iron to induce intracellular PrP conversion over copper because of the pathological implications of its accumulation in prion diseases. We found that Fe(III) played a role in the induction of internalized rPrP accumulation and rPrP conversion to proteinase K (PK)-resistant PrP (PrP^{res}). Moreover, an intact cell structure, including dynamic vesicular fusion in endosomal trafficking, appeared to be critical for Fe(III)-induced PrP^{res} generation.

2. Materials and methods

2.1. Generation of recombinant protein

rPrP corresponding to amino acids 24–241 of bovine PrP was cloned and expressed in *Escherichia coli* BL21 (DE3) after induction with 1 mM IPTG for 14 h. Cells were resuspended in cold PBS containing 5 mM EDTA and a protease inhibitor cocktail and then sonicated. Inclusion bodies were solubilized with buffer A (20 mM sodium phosphate, pH 7.4, 6 M GdnHCl, 20 mM imidazole, 0.5 M NaCl). After brief sonication, the solubilized proteins were collected by centrifugation. Clear lysates were loaded onto a HiTrap Chelating HP column (GE Healthcare, WI, USA), and purification

* Corresponding author. Address: College of Veterinary Medicine, Seoul National University, 1 Gwanak-ro, Gwanak-gu, Seoul 151-742, Korea. Fax: +82 2 877 8284.
E-mail address: hjwoo@snu.ac.kr (H.-J. Woo).

0006-291X/$ - see front matter © 2013 Elsevier Inc. All rights reserved.
http://dx.doi.org/10.1016/j.bbrc.2013.02.021

was performed according to the manufacturer's instructions. Fractions were dialyzed against 50 mM sodium acetate, pH 5.0, containing 5% glycerol, and then re-dialyzed against 20 mM HEPES, pH 7.4.

2.2. Cell culture, exposure to iron, and rPrP treatment

The HpL3-4 cell line from hippocampal cells of PrP-deficient mice [13] was kindly provided by Prof. Yong-Sun Kim (Hallym University, Korea) with the permission of Prof. Takashi Onodera (University of Tokyo, Japan). In a typical experiment, cells were plated at a density of 0.3×10^5 cells/mL. The cells were exposed to either 0.3 mM ferrous chloride ($FeCl_2$) [Fe(II)] or 0.6 mM ferric ammonium citrate (FAC) [Fe(III)] for 24 h. Subsequently, 0.6 μM rPrP was added for an additional 24 h. For other trivalent metal ion exposures, 0.6 mM aluminum chloride [Al(III)] and chromium chloride [Cr(III)] were used.

2.3. Detergent solubility and proteinase K resistance of intracellular rPrP

Cells were collected and lysed in lysis buffer B (20 mM Tris–HCl, pH 8, 130 mM NaCl, 2 mM EDTA, 0.5% Triton X-100, 0.5% NP-40, 0.2% sodium deoxycholate, protease inhibitor cocktail, 0.1 mM PMSF), and large debris was removed by brief centrifugation. The supernatants were then subjected to centrifugation at 16,000*g* for 45 min. Samples from resuspended pellets, as well as supernatants, were subjected to SDS–PAGE. In the PK digestion assay, cells were lysed in buffer B without protease inhibitors. In a typical experiment, digestion was performed by treating protein of each sample (1 mg/mL) with 5 μg/mL of PK at 37 °C for 30 min. The reaction was stopped by addition of 2 mM PMSF.

2.4. Treatment with U18666A and NH_4Cl

U18666A (Enzo Life Sciences, NY, USA) was reconstructed according to manufacturer's instructions and used at 3 μM concentration. Cells exposed to Fe(II) or Fe(III) were subsequently treated with U18666A for 24 h. Subsequently, 0.6 μM rPrP was added for another 24 h. For NH_4Cl treatment, 20 mM NH_4Cl was added 30 min prior to rPrP treatment. To analyze changes in the formation of PK-resistant PrP, cell lysates were either treated or not treated with 5 μg/mL PK.

2.5. Immunoblotting

Immunoblotting was performed for detecting PrP and other proteins. Primary anti-PrP antibody 1E4 (1:6000), anti-lamin A/C antibody (1:7000), or β-actin antibody (1:5000) was used, followed by appropriate secondary antibodies (Supplementary data). The blots were developed by enhanced chemiluminescence (GE Healthcare, WI, USA). The relative intensity of the proteins was analyzed using ImageJ analysis (National Institutes of Health, MD, USA).

2.6. Statistical analysis

All experiments were repeated 3 times. The results are expressed as the mean ± standard deviation (SD). Statistical analysis was performed by Tukey's test for comparing multiple groups, using SPSS software (SPSS Inc., IL, USA). Differences were considered significant at $p < 0.01$.

3. Results

3.1. Internalized rPrP accumulates upon Fe(III) exposure

The cytotoxicity in 2 oxidation states of iron ($FeCl_2$ and FAC) over a range of concentrations (0.3–2.4 mM) was examined, and an optimal concentration of iron exposure was selected (Supplementary data). Treatment of cells with purified rPrP alone at 0.6 μM had no effect on cell viability (data not shown). To assess the effects of iron on the internalized rPrP, cells were exposed to 0.3–1.2 mM of either $FeCl_2$ or FAC. The internalized rPrP from whole-cell lysates was detected with 1E4 antibody. The levels of internalized rPrP were iron concentration-dependent (Fig. 1A). Fe(III) exposure induced as much as 13-fold more internalized rPrP compared with the mock-exposed control (Fig. 1B, lane 5; Fig. 1C). Interestingly, cells with Fe(II) exposure showed only a marginal increase in the levels of internalized rPrP compared with the control (Fig. 1B, lane 4; Fig. 1C). No signals were detected from the cells without rPrP treatment (Fig. 1B, lane 2), indicating the absence of endogenous PrP^C in HpL3-4 cells.

To define the time-dependent intracellular accumulation of rPrP in response to iron, rPrP was added to cells for 4, 8, 16, and 24 h. In cells exposed to Fe(III), the level of rPrP was low early after its addition (Fig. 1D, lane 9), but it increased dramatically over time (Fig. 1D, lanes 10–12). Although cells exposed to Fe(II) showed an increase in rPrP up to 16 h of incubation, this increase was marginal, and the levels eventually returned to those observed in the control (Fig. 1D, lanes 5–8).

To clarify whether this rPrP accumulation is specific to Fe(III) itself or to trivalency *per se*, exposures to other trivalent metal ions, including Al(III) and Cr(III), were performed (Fig. 1E). A large increase in rPrP levels was observed only in the cells exposed to Fe(III) (Fig. 1E, lane 3), and neither Al(III) nor Cr(III) induced the increase in rPrP levels.

To verify whether the Fe(III)-mediated increase of intracellular rPrP was specific to rPrP, we treated cells with 0.6 μM of recombinant human galectin-3 (rGal-3), which has a similar molecular mass (29 kDa) to rPrP. The level of internalized rGal-3 did not increase in Fe(III)-exposed cells compared with the control cells (Fig. 1F, lanes 3 and 4). Endogenous galectin-3 in HpL3-4 cells showed a slightly higher molecular mass (ca. 30 kDa), and its expression was similar in both mock and Fe(III)-exposed cells.

3.2. Detergent solubility and PK resistance of internalized rPrP

The detergent solubility assay is commonly used to distinguish PrP^{Sc}-like characteristics from PrP^C. Internalized rPrP was detected mainly in the insoluble fraction treated with Fe(III) (Fig. 2A, lane 6), whereas lamin A/C, a nuclear membrane protein, was found in the soluble fraction, regardless of iron exposure (Fig. 2A).

Resistance to PK is considered a hallmark discriminator of PrP^{Sc} from PrP^C. To assess whether rPrP in cells was converted to PrP^{Sc} by iron exposure, resistance of internalized rPrP against PK digestion was measured (Fig 2B). rPrP from Fe(III)-exposed cells showed partial PK resistance, and we designated this rPrP as PrP^{res} (Fig. 2B, lanes 9–12). As the concentration of PK increased, intact rPrP (25 kDa) was digested, yielding a PK-resistant fragment (17 kDa). However, rPrP from the control and Fe(II)-exposed cells was completely degraded at a minimal PK concentration of 1 μg/mL (Fig. 2B, lane 6). To define a direct interaction of Fe(III) and rPrP for PrP^{res} formation without subcellular structures, 0.6 μM rPrP in HEPES buffer was added to cell lysates treated with iron *in vitro*. The immunoblots revealed that a simple biophysical reaction between rPrP and Fe(III) or cellular components was not sufficient to obtain

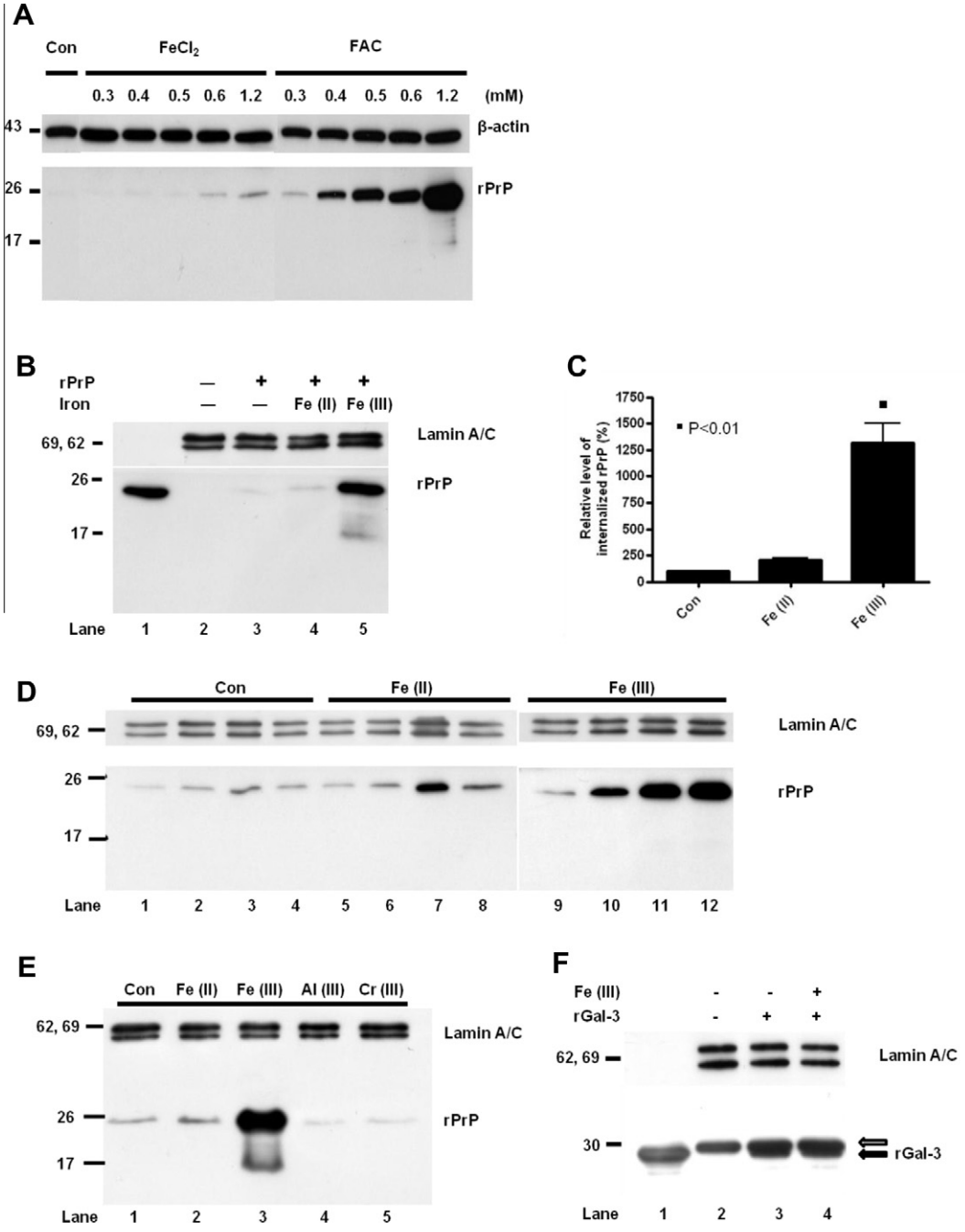

Fig. 1. Accumulation of internalized recombinant prion protein (rPrP) induced by Fe(III) exposure. (A) Cells were exposed to 0.3–1.2 mM $FeCl_2$ or FAC for 24 h. Subsequently, 0.6 μM rPrP was added for another 24 h. rPrP was detected by the anti-prion protein antibody 1E4. The levels of internalized rPrP were FAC concentration-dependent. (B) Detection of internalized rPrP from mock-exposed (lane 3), Fe(II)-exposed (lane 4), or Fe(III)- exposed (lane 5) lysates. Purified rPrP (200 ng) was loaded in lane 1. In the absence of rPrP, no signal was detected from cell lysates (lane 2). (C) Quantification of internalized rPrP showed a greater increase in the level of rPrP in cells exposed to Fe(III) than in the control. The values shown are a percentage of the rPrP level in the control with metal exposures (mean ± SD). The statistical significance between the experimental group and control is shown as ■ ($p < 0.01$). (D) Detection of rPrP from cells treated with rPrP for 4 h (lanes 1, 5, and 9), 8 h (lanes 2, 6, and 10), 16 h (lanes 3, 7, and 11), or 24 h (lanes 4, 8, and 12) showed a time-dependent pattern of intracellular rPrP accumulation with Fe(III) exposure. (E) Other trivalent metal ions, Al(III) and Cr(III), did not induce an increase in the level of rPrP in cells (lanes 4 or 5). (F) Other recombinant proteins, such as recombinant galectin-3 (rGal-3, which has a similar MW to rPrP), did not accumulate upon Fe(III) exposure. Purified rGal-3 (50 ng, lane 1) was loaded to distinguish the internalized rGal-3 from the endogenous galectin-3 (Gal-3).

PrP^{res}, suggesting that an intact cell structure was required for PrP^{res} generation (Fig. 2C).

3.3. Fe(III)-mediated conversion occurred in vesicular trafficking

Development of PrP^{res} was examined by the inhibition of cellular processes or sites associated with rPrP metabolism. U18666A is known to effectively inhibit vesicular trafficking, thereby preventing protein degradation [14]. Following drug treatment, complete disappearance of PrP^{res} was observed upon PK digestion, although a high level of rPrP was detected in Fe(III)-exposed cells without PK treatment (Fig. 3A).

The importance of the acidic environment of lysosomes in the formation of PrP^{res} was tested using NH_4Cl, an inhibitor of endolysosomal acidification that results in impairment of the lysosomal degradation system [15]. In the presence of Fe(III), no effect of pre-

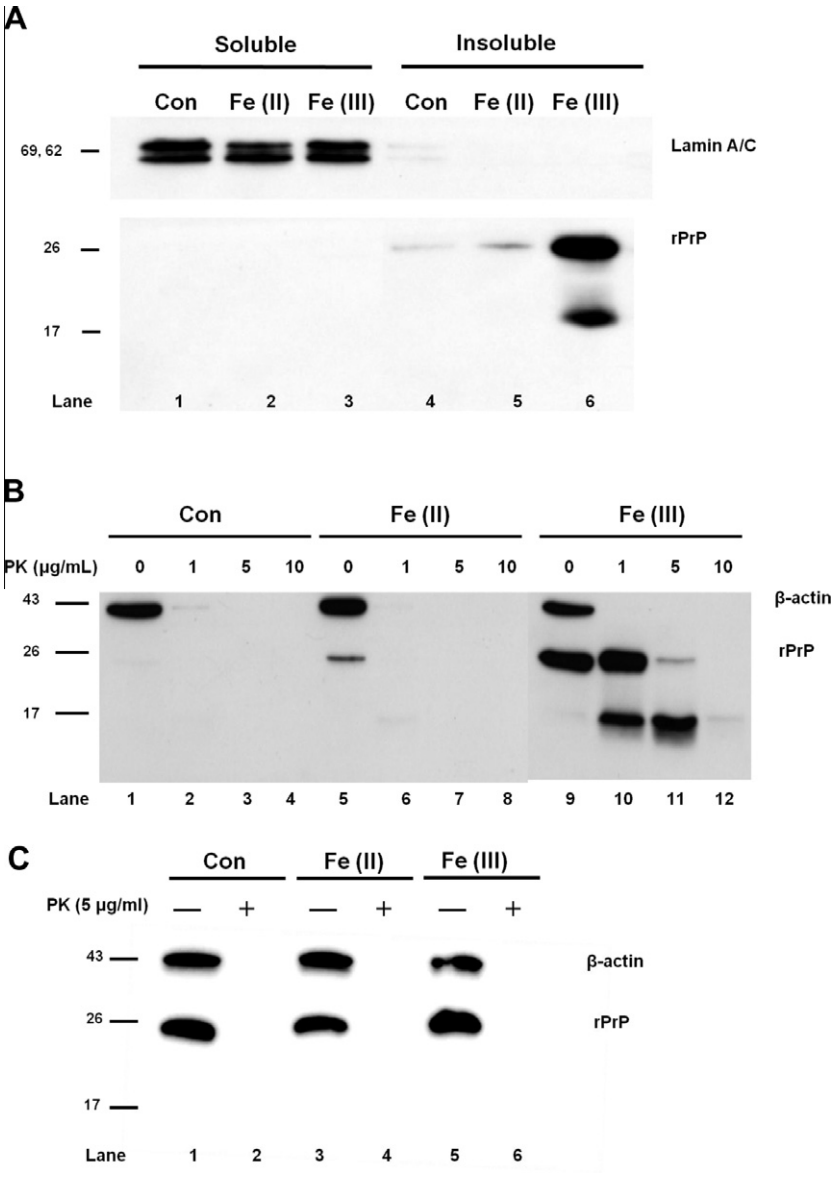

Fig. 2. Detergent insolubility and proteinase K (PK) resistance of internalized rPrP induced by Fe(III). (A) Cells exposed to iron for 24 h were treated with rPrP (0.6 μM) for another 24 h. Cells were then lysed in 0.25% SDS-containing lysis buffer. The soluble supernatant (lanes 1–3) and insoluble pellet (lanes 4–6) were subjected to SDS–PAGE and immunoblotting. Internalized rPrP was largely detected only in the Fe(III)-exposed insoluble fraction (lane 6). (B) Conversion from rPrP to PrP^{res} in the cellular context was confirmed by PK treatment (1, 5, and 10 μg/mL) for 30 min at 37 °C. From cells exposed to Fe(III), both intact (25 kDa) and PrP^{res} (17 kDa) fragments were detected at 5 μg/mL PK (lane 11). (C) The reaction between iron and rPrP (0.6 μM in 20 mM HEPES, pH 7.4) in cell lysates *in vitro*. rPrP (20 μg/mL) incubated with either Fe(II) or Fe(III) was completely digested by PK treatment at 5 μg/mL of rPrP (lanes 2, 4, and 6).

treatment with 20 mM of NH_4Cl on PrP^{res} expression was found, suggesting that endolysosomal acidification might not be important in the cellular process for PrP^{res} (Fig. 3B).

4. Discussion

In previous studies on prion-infected cells and brains, iron has been implicated in prion pathology [3,10,16], although the contribution of the 2 oxidative states of iron has not been elucidated. In this study, we investigated whether internalized rPrP was converted into PrP^{res} by Fe(II) and Fe(III) during vesicular trafficking in PrP-deficient HpL3-4 cells. Intracellular accumulation and conversion of rPrP was specifically induced by Fe(III), but not by Fe(II), although both iron states are believed to participate in prion diseases (Fig. 1). Other trivalent metal ions failed to induce PrP accumulation, and the accumulation of another internalized recombinant protein (rGal-3) was not increased by Fe(III) (Fig. 1E and F). These data indicate that the increase in rPrP is due to a specific biochemical effect of Fe(III) on rPrP. Das et al. [8] and Basu et al. [9] reported that $FeCl_2$ and FAC induced a conformational change of PrP into detergent-insoluble and/or PK-resistant isoforms when exposed to cells that overexpressed endogenous PrP^{C}. The authors interpreted this change as formation of ferritin–PrP coaggregates in lysosomes, which conferred PrP with PK resistance and detergent insolubility [8,9,17]. However, ferritin upregulation and the formation of PrP coaggregates occurred whenever the cells were exposed to iron, regardless of the cationic valence state of iron [8,9]. In contrast, our results suggest that additional factors are at play. There are at least 2 explanations that may account for the differential PrP accumulation induced by Fe(III) rather than Fe(II). First, distinct molecular mechanisms of intracellular iron

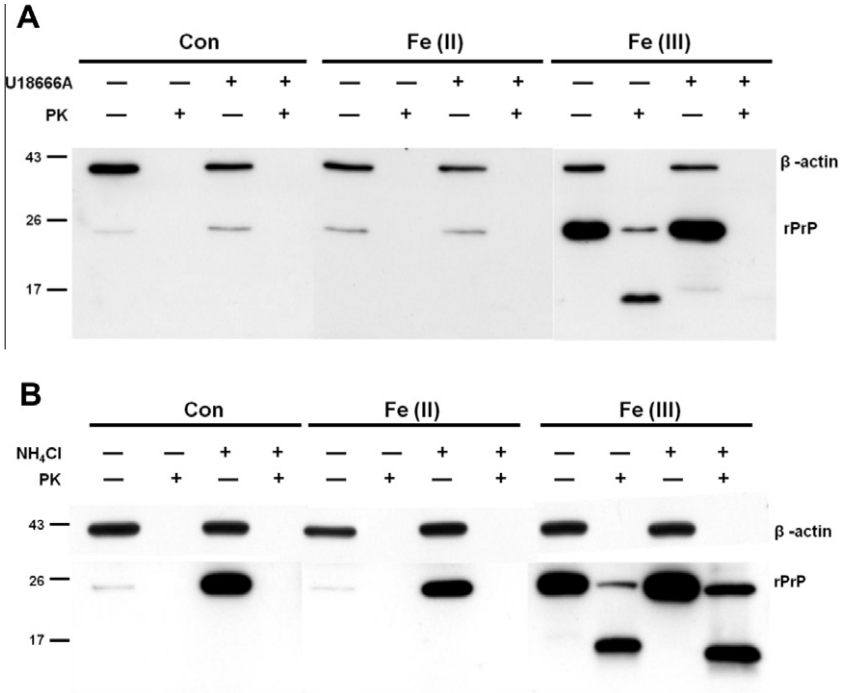

Fig. 3. Reduction of PrP^{res} by U18666A but not by NH_4Cl. Levels of internalized rPrP and PrP^{res} after U18666A (A) or NH_4Cl (B) treatment were analyzed by immunoblotting. Cells exposed to Fe(II) or Fe(III) were treated with (+) or without (−) 3 μM U18666A for 24 h or 20 mM NH_4Cl for 30 min. PK was used at 5 μg/mL (PK+) or not (PK−). (A) Under U18666A treatment, a decrease in Fe(III)-induced PrP^{res} was observed. (B) NH_4Cl treatment did not affect the generation of PrP^{res} by Fe(III).

transport might depend on the oxidative state of iron; particular examples are vesicular and non-vesicular iron import [27]. Cellular uptake of Fe(III) occurs via the receptor-mediated endocytosis of transferrin (Tf). The Fe(III)–Tf complex then binds to a specific membrane-bound transferrin receptor (TfR). Uptake of Fe(II), on the other hand, is mediated by plasma membrane-localized iron importers such as the divalent metal transporter 1 (DMT1) and transient receptor potential mucolipin 1 (TRPML1). The similar transportation route of both internalized rPrP and Fe(III) within vesicles might provide an environment conducive to PrP conversion.

Second, given that the affinity of PrP for iron is still unknown, Fe(II) and Fe(III) may have different affinities for rPrP. Although previous studies have been shown that Fe(III), but not Fe(II), binds to PrP, these studies have been limited to *in vitro* experiments with rPrP [5,9]. Therefore, the possibility that other intracellular factor(s) in vesicular trafficking might also be affected by Fe(III) cannot be excluded. Although many questions remain regarding the conversion of rPrP to PrP^{res}, the result from the cell lysates in our study clearly demonstrates that Fe(III)-mediated PrP^{res} conversion was neither from a direct contact between rPrP and Fe(III), nor from a simple biochemical reaction between intracellular elements; rather, it required a complex cellular milieu, including an intact cellular structure (Fig. 2C). Moreover, these findings were not specific to the PrP^{C}-deficient cell line, as the same observations were obtained in GT1–7, a PrP^{C}-expressing cell line (data not shown). The experimental system used in this study was focused on the specific role of Fe(II) or Fe(III) on the PrP alteration. Considering the natural feature and metabolic pathway of endogenous prion protein and iron, it was in the limited condition using rPrP and the excessive amount of iron. However, our system seems to be appropriate to provide the simplicity and specificity to evaluate the role of Fe(III) in accumulation and conversion of the internalized prion protein.

Assessment of the PK resistance of rPrP after treatment with U18666A or NH_4Cl demonstrated that vesicular trafficking, rather than acidic lysosomes, is the critical process required for Fe(III)-associated PrP conversion (Fig. 3). Notably, the ability of U18666A to reduce PrP^{res} levels indicated inhibition of PrP^{res} formation. U18666A is known to induce cholesterol accumulation and consequently inhibit a broad range of vesicular trafficking [18,19]. Since endocytosed and intracellular components within vesicles dynamically transit through homotypic and heterotypic membrane fusions along the pathway leading to lysosomes [20], a factor(s) present in vesicles would be required for the endocytosed rPrP to obtain PK resistance. The observation that cholesterol depletion reduced PrP^{Sc} levels underscores the importance of a lipid environment for PrP conversion [21,22]. This phenomenon has been explained by the inability of PrP^{C} to associate with lipid rafts, which in turn reduces the cell surface expression of PrP^{C} [23]. Although U18666A, which inhibits cholesterol recycling, also impairs PrP^{Sc} propagation, it does not affect the interaction between PrP^{C} and lipid rafts [24,25]. Moreover, HpL3-4 cells are PrP^{C}-deficient; thus, cell surface expression of PrP^{C} does not seem to be required either for U18666A-mediated PrP^{res} reduction or for Fe(III)-associated PrP^{res} generation under our experimental conditions. This is only a simple study which is not sufficient to explain the complicated trafficking pathway of PrP conversion. A series of fine experiments including fluorescence microscopy with tracers and/or co-localization with other cellular markers will be useful to identify more details on trafficking pathways for PrP conversion in physiological condition.

Although the amounts of iron added to the cells were excessive compared with the levels found in diseased brains or in other iron-overloaded cell models [8,9], our experimental system recapitulated PrP^{Sc}-like features, including partial PK resistance and insolubility; this presumably corresponds to the recombinant PrP^{res}, converted by PrP^{Sc} derived from prion-infected brains [26,27], resulting in a useful tool for the study of the intracellular mechanisms of PrP conversion. Considering that not only normal aged brains but also brains with other neurodegenerative diseases, including Alzheimer's disease and Parkinson's disease, exhibit

abnormal iron accumulation [28], this experimental approach can provide insight into the potential roles of iron in protein-misfolding diseases.

Acknowledgments

This work was supported by a Grant (No. 2012E5200400) from the Korea Centers for Disease Control and Prevention (KCDC), Ministry of Health and Welfare, Korea.

Appendix A. Supplementary data

Supplementary data associated with this article can be found, in the online version, at http://dx.doi.org/10.1016/j.bbrc.2013.02.021.

References

[1] J. Collinge, Prion diseases of humans and animals: their causes and molecular basis, Annu. Rev. Neurosci. 24 (2001) 519–550.
[2] N. Singh, A. Singh, D. Das, M.L. Mohan, Redox control of prion and disease pathogenesis, Antioxid. Redox Signal. 12 (2010) 1271–1294.
[3] S. Fernaeus, T. Land, Increased iron-induced oxidative stress and toxicity in scrapie-infected neuroblastoma cells, Neurosci. Lett. 382 (2005) 217–220.
[4] A. Singh, M.L. Mohan, A.O. Isaac, X. Luo, J. Petrak, D. Vyoral, N. Singh, Prion protein modulates cellular iron uptake: a novel function with implications for prion disease pathogenesis, PLoS ONE 4 (2009) e4468.
[5] D.R. Brown, F. Hafiz, L.L. Glasssmith, B.S. Wong, I.M. Jones, C. Clive, S.J. Haswell, Consequences of manganese replacement of copper for prion protein function and proteinase resistance, EMBO J. 19 (2000) 1180–1186.
[6] A.M. Thackray, R. Knight, S.J. Haswell, R. Bujdoso, D.R. Brown, Metal imbalance and compromised antioxidant function are early changes in prion disease, Biochem. J. 362 (2002) 253–258.
[7] S. Fernaeus, J. Halldin, K. Bedecs, T. Land, Changed iron regulation in scrapie-infected neuroblastoma cells, Brain Res. Mol. Brain Res. 133 (2005) 266–273.
[8] D. Das, X. Luo, A. Singh, Y. Gu, S. Ghosh, C.K. Mukhopadhyay, S.G. Chen, M.S. Sy, Q. Kong, N. Singh, Paradoxical role of prion protein aggregates in redox-iron induced toxicity, PLoS ONE 5 (2010) e11420.
[9] S. Basu, M.L. Mohan, X. Luo, B. Kundu, Q. Kong, N. Singh, Modulation of proteinase K-resistant prion protein in cells and infectious brain homogenate by redox iron: implications for prion replication and disease pathogenesis, Mol. Biol. Cell 18 (2007) 3302–3312.
[10] A. Singh, A.O. Isaac, X. Luo, M.L. Mohan, M.L. Cohen, F. Chen, Q. Kong, J. Bartz, N. Singh, Abnormal brain iron homeostasis in human and animal prion disorders, PLoS Pathog. 5 (2009) e1000336.
[11] G.G. Kovacs, E. Gelpi, T. Strobel, G. Ricken, J.R. Nyengaard, H. Bernheimer, H. Budka, Involvement of the endosomal-lysosomal system correlates with regional pathology in Creutzfeldt–Jakob disease, J. Neuropathol. Exp. Neurol. 66 (2007) 628–636.
[12] R. Goold, S. Rabbanian, L. Sutton, R. Andre, P. Arora, J. Moonga, A.R. Clarke, G. Schiavo, P. Jat, J. Collinge, S.J. Tabrizi, Rapid cell-surface prion protein conversion revealed using a novel cell system, Nat. Commun. 2 (2011) 281.
[13] C. Kuwahara, A.M. Takeuchi, T. Nishimura, K. Haraguchi, A. Kubosaki, Y. Matsumoto, K. Saeki, T. Yokoyama, S. Itohara, T. Onodera, Prions prevent neuronal cell-line death, Nature 400 (1999) 225–226.
[14] R.J. Cenedella, Cholesterol synthesis inhibitor U18666A and the role of sterol metabolism and trafficking in numerous pathophysiological processes, Lipids 44 (2009) 477–487.
[15] G. Misinzo, P.L. Delputte, H.J. Nauwynck, Inhibition of endosome–lysosome system acidification enhances porcine circovirus 2 infection of porcine epithelial cells, J. Virol. 82 (2008) 1128–1135.
[16] R.B. Petersen, S.L. Siedlak, H.G. Lee, Y.S. Kim, A. Nunomura, F. Tagliavini, B. Ghetti, P. Cras, P.I. Moreira, R.J. Castellani, M. Guentchev, H. Budka, J.W. Ironside, P. Gambetti, M.A. Smith, G. Perry, Redox metals and oxidative abnormalities in human prion diseases, Acta Neuropathol. 110 (2005) 232–238.
[17] N. Singh, D. Das, A. Singh, M.L. Mohan, Prion protein and metal interaction: physiological and pathological implications, Curr. Issues Mol. Biol. 12 (2009) 99–108.
[18] L.W. Jin, F.S. Shie, I. Maezawa, I. Vincent, T. Bird, Intracellular accumulation of amyloidogenic fragments of amyloid-beta precursor protein in neurons with Niemann–Pick type C defects is associated with endosomal abnormalities, Am. J. Pathol. 164 (2004) 975–985.
[19] K. Sobo, I. Le Blanc, P.P. Luyet, M. Fivaz, C. Ferguson, R.G. Parton, J. Gruenberg, F.G. van der Goot, Late endosomal cholesterol accumulation leads to impaired intra-endosomal trafficking, PLoS ONE 2 (2007) e851.
[20] F.G. van der Goot, J. Gruenberg, Intra-endosomal membrane traffic, Trends Cell Biol. 16 (2006) 514–521.
[21] C. Bate, M. Salmona, L. Diomede, A. Williams, Squalestatin cures prion-infected neurons and protects against prion neurotoxicity, J. Biol. Chem. 279 (2004) 14983–14990.
[22] A. Mange, N. Nishida, O. Milhavet, H.E. McMahon, D. Casanova, S. Lehmann, Amphotericin B inhibits the generation of the scrapie isoform of the prion protein in infected cultures, J. Virol. 74 (2000) 3135–3140.
[23] S. Gilch, C. Kehler, H.M. Schatzl, The prion protein requires cholesterol for cell surface localization, Mol. Cell. Neurosci. 31 (2006) 346–353.
[24] Z. Marijanovic, A. Caputo, V. Campana, C. Zurzolo, Identification of an intracellular site of prion conversion, PLoS Pathog. 5 (2009) e1000426.
[25] S. Gilch, C. Bach, G. Lutzny, I. Vorberg, H.M. Schatzl, Inhibition of cholesterol recycling impairs cellular PrP(Sc) propagation, Cell. Mol. Life Sci. 66 (2009) 3979–3991.
[26] R. Atarashi, J.M. Wilham, L. Christensen, A.G. Hughson, R.A. Moore, L.M. Johnson, H.A. Onwubiko, S.A. Priola, B. Caughey, Simplified ultrasensitive prion detection by recombinant PrP conversion with shaking, Nat. Methods 5 (2008) 211–212.
[27] M. Eiden, G.J. Palm, W. Hinrichs, U. Matthey, R. Zahn, M.H. Groschup, Synergistic and strain-specific effects of bovine spongiform encephalopathy and scrapie prions in the cell-free conversion of recombinant prion protein, J. Gen. Virol. 87 (2006) 3753–3761.
[28] E. Mills, X.P. Dong, F. Wang, H. Xu, Mechanisms of brain iron transport: insight into neurodegeneration and CNS disorders, Future Med. Chem. 2 (2010) 51–64.